Malaysian Journal of Analytical Sciences, Vol 26 No 3 (2022): 664 - 683

Malaysian Journal of Analytical Sciences (MJAS)
Published by Malaysian Analytical Sciences Society

ENHANCING THE OXYGEN REDUCTION REACTION OF LOW-PLATINUM AND NON-PLATINUM CATALYSTS FOR FUEL CELL APPLICATIONS

(Peningkatan Tindak Balas Penurunan Oksigen Mangkin Platinum Bermuatan Rendah dan Bebas Platinum Untuk Aplikasi Sel Bahan Api)

Kazi Rumanna Rahman[1], Kuan Ying Kok[2], Nor Azillah Fatimah Othman[3], Wai Yin Wong[1], Kean Long Lim[1]*

[1]Fuel Cell Institute,
Universiti Kebangsaan Malaysia, 43600 UKM Bangi, Selangor, Malaysia
[2] Industrial Technology Division
[3]Radiation Processing Technology Division
Malaysia Nuclear Agency, 43000, Kajang, Selangor, Malaysia

**Corresponding author email: kllim@ukm.edu.my*

Received: 13 December 2021; Accepted: 6 March 2022; Published: 27 June 2022

Abstract

Nowadays, research efforts are focused on developing low-Pt and non-Pt catalysts for ORR. The addition of Pt-group metal (PGM) in pure Pt to form Pt-PGM catalysts exhibits better ORR performance than pure PGM catalysts and Pt/C. More than 20 wt.% of Pt loading is required in Pt-PGM alloys for improving catalytic activity. Studies have also shown that the addition of transition metal (TM), which has a smaller atomic size, into PGM reduced the bond distance between two metallic atoms and geometric parameters, thus remarkably improving the catalytic stability and ORR activity. However, TM based catalysts should be supported on nitrogen-doped carbon with high surface area to attain high ORR activity. A large surface area and high electronic conductivity of carbon support also facilitate the ORR activity. Performances of alloy catalysts are directly related to their synthesis temperature and structural properties. Designing the core-shell combinations and controlling the shell thickness is one of the structural strategies in enhancing mass activity and durability. Lately, irradiation techniques are used to modify the physicochemical properties. Nevertheless, TM-based catalysts are usually stable in alkaline solutions but not in acidic solutions. This review focuses on the strategies to develop cost-effective catalysts from low-platinum and non-platinum catalysts with enhanced ORR activity.

Keywords: oxygen reduction reaction, platinum group metal alloys, transition metal catalysts, synthesis techniques

Abstrak

Pada masa kini, usaha penyelidikan tertumpu kepada pembangunan mangkin platinum (Pt) bermuatan rendah dan bebas platinum untuk tindak balas penurunan oksigen (ORR). Penambahan logam kumpulan Pt (PGM) dalam Pt tulen untuk membentuk Pt-PGM menunjukkan prestasi ORR yang lebih baik daripada prestasi mangkin PGM tulen dan Pt/C. Sebanyak lebih daripada 20 wt.% muatan Pt adalah diperlukan dalam aloi Pt-PGM untuk meningkatkan aktiviti pemangkinan. Kajian telah menunjukkan penambahan logam peralihan (TM) yang mempunyai saiz atom yang lebih kecil ke dalam PGM mengurangkan jarak antara dua atom logam dan parameter geometri sekali gus meningkatkan kestabilan pemangkinan dan aktiviti ORR. Namun demikian, mangkin berasakan TM perlu disokong dengan karbon terdop nitrogen yang berpermukaan yang luas untuk mencapai aktiviti ORR yang tinggi. Penyokong karbon yang berpemukaan luas dan mempunyai kekonduksian elektronik yang tinggi juga memudahkan aktiviti ORR. Prestasi mangkin aloi adalah berkait langsung dengan suhu sintensi dan sifat strukturnya. Mereka bentuk gabungan teras-cangkerang dan mengawal ketebalan cangkerang adalah salah satu strategik penstrukturan dalam meningkatkan aktiviti jisim dan ketahanan. Akhir-akhir ini, teknik-teknik penyinaran digunakan ubah mengubahsuai sifat fizikokimia. Namun demikian, mangkin berasaskan TM biasanya stabil dalam larutan alkali tetapi tidak dalam larutan asid. Ulasan ini berfokus pada strategik untuk membangunkan magkin berkos efektif daripada mangkin Pt bermuatan rendah dan bebas platinum dengan aktitiviti ORR yang dipertingkatkan.

Kata kunci: tindak balas penurunan oksigen, logam aloi kumpulan platinum, mangkin logam peralihan, kaedah sintesis

Introduction

A fuel cell is an energy conversion device that converts chemical energy into electric energy through an oxidation reaction at the anode and a reduction reaction at the cathode. The cathode reaction, known as oxygen reduction reaction (ORR), is a fundamental reaction to various disciplines, such as energy conversion, material dissolution, or biology. The performance of fuel cells depends on the rate of ORR [1, 2]. Difficulties in O_2 adsorption, O-O bond cleavage and oxide removal are the main reasons for the sluggish reaction kinetics of ORR [3]. The state-of-the-art Pt/C (platinum/carbon black) catalyst and Pt-based alloy catalysts are used for the cathode reaction in aqueous electrolytes, and these catalysts are considered the best for ORR. All Pt or Pt-based catalysts still suffer from CO and S poisoning on Pt, loss of active surface area, corrosion of carbon support, low durability and limited supply, high cost, and use of a high amount of Pt [4–6]. So, non-Pt based catalysts with improved catalytic activity are required to overcome these limitations of Pt [7]. The main characteristic of an effective fuel cell catalyst is its capability to facilitate the rate of ORR [8]. Transition metal (TM) alloys, chalcogenides, carbides, nitrides, and metal-N4 macrocyclic compounds instead of Pt/C and PGM catalysts, are potential electrocatalysts for ORR [9]. Composition, particle size, crystallographic orientation, etc contribute to the enhancement in catalytic activity and d-band vacancy is considered as an important factor for enhancing catalytic behavior towards ORR. For developing a cost effective catalyst with improving ORR activity, the current research follows four different trends: 1) to reduce the wt% of Pt in alloy catalysts, 2) to develop the PGM free catalyst named M-N-C, where M for transition metal, nitrogen, and carbon, 3) to utilize the carbon with large surface area as catalyst support and 4) synthesis technique for designing cost-effective ORR cathode catalysts[10–13]. In the following section, we describe the general mechanism of ORR cathode in acidic and alkaline solutions, which gives a clear idea of the reaction paths.

General mechanism of ORR cathode

In general, anode and cathode reactions occur on a metal surface. The reaction that occurs at the cathode site is known as the ORR reaction. Usually, the ORR reaction is the limiting reaction step of the overall reaction because of its sluggish kinetic, hence it is essential to understand the ORR mechanisms to design an effective catalyst.

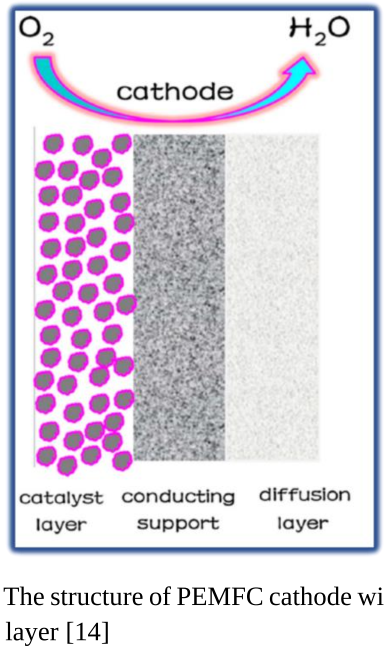

Figure 1. The structure of PEMFC cathode with catalyst layer [14]

The ORR mechanism involves a direct four-electron (4e-) or a series of two-electron (2e-) pathways. A one-step 4e- transfer mechanism is more efficient than a 2e- transfer mechanism. Thus, catalysts that facilitate the 4e- pathway reaction are more favorable. In the $4e^-$ transfer pathway, O_2 is converted into either H_2O (acidic medium) or OH^- (alkaline medium) on a single catalytic site. This process depends completely on the electrolytes [14–17].

In an acidic electrolyte, the $4e^-$ transfer pathway can be written as in Eq. (1):

$$O_2\,(g) + 4H^+\,(aq) + 4e^- \rightarrow 2H_2O(l) \qquad (1)$$

and $2e^-$ transfer pathway can be expressed as Eqs. (2, 3, and 4):

$$O_2\,(g) + 2H^+\,(aq) + 2e^- \rightarrow H_2O_2\,(l) \qquad (2)$$

H_2O_2 is produced in the intermediate step of the Eq.(2) pathway. H_2O_2 is finally reduced to water:

$$H_2O_2\,(aq) + 2H^+\,(aq) + 2e^- \rightarrow 2H_2O\,(l) \qquad (3)$$

or is decomposed as follows:

$$H_2O_2(aq) + 2H(aq) + 2e^- \rightarrow 2H_2O(l) + O_2(g) \qquad (4)$$

On the other hand, O_2 is converted into OH^- by $4e^-$ pathway, which is written as Eq. (5), and forms HO_2^- via $2e^-$ pathway in an alkaline medium,

$$O_2\,(g) + 2H_2O\,(aq) + 4e^- \rightarrow 4OH^-\,(l) \qquad (5)$$

Eqs. (6,7 and 8) express the step of the $2e^-$ transfer pathway alkaline solutions.

$$O_2\,(g) + H_2O\,(aq) + 2e^- \rightarrow HO_2^-\,(l) + HO^- \qquad (6)$$

Peroxide is also unstable

$$HO_2^-\,(aq) + H_2O\,(l) + 2e^- \rightarrow 3OH^-\,(aq) \qquad (7)$$

and decomposes into the following:

$$2HO_2^-\,(aq) \rightarrow 2HO^-\,(aq) + O_2(g) \qquad (8)$$

Pt-group alloy catalysts

Pt is the best monometallic catalyst for ORR in acidic and alkaline solutions. The fuel cell stack needs almost 80%–90% Pt, which increases the cost of the entire stack. Moreover, Pt has some drawbacks, such as CO poisoning, short life span, low durability, etc. So, the current research trend emphasizes reducing Pt use and the development of bimetallic and trimetallic alloy catalysts to overcome the stumbling block of Pt [18–20]. Some researchers used several noble metals like Pd, Ir, Rh, Ag, and Ru as cathode catalysts. All single noble metal catalysts followed the $4e^-$ pathway but exhibited lower catalytic activity than Pt. Improvement of catalytic activity depends on the optimization of particle size and shape, surface structure, support metal, and synthesis process [21]. It also revealed that combinations of two Pt-group metals can tune the ability of oxygen adsorption due to constructing a hetero-metal-metal bond by altering the electronic configurations. Coupled metals also generate a new active site. The mutual effect of changing electronic and geometric structure encourages a $4e^-$ reaction pathway towards ORR [17]. The d band vacancies which consider as important parameters increase due to the existence of Pt atom, d band vacancies boosted 2π electron donation from O_2 to the catalyst surface. Finally, O_2 reacted with donated electrons and protons to yield desirable H_2O molecules [22].

Due to the similar crystal structure of Pt, palladium-based catalysts have stimulated extensive concern among researchers [23]. Zhou et al. reported that Pt-Pd/C exhibited higher durability than commercial Pt/C as a cathode catalyst. They also concluded that particle size and electrochemical surface area (ECSA) loss are associated with durability, and larger particles are more stable in alkaline solution [24]. Wang et al. established the relationship between weight ratio and particle size. They reported that ORR activity was controlled by the size of Pt nanoparticles, and 30% of Pt-Pd/C exhibited remarkable performances, whereas the weight ratio of Pt: Pd was 1:1. The mass activity (MA) and the ECSA value of this Pt-Pd/C catalyst (MA= 0.488 mA μg^{-1} and ECSA=107.7 $m^2\,g^{-1}$) are four times and 1.69 times higher than those of commercial 10% Pt/C (MA=0.123 mA μg^{-1} and ECSA=63.6 $m^2\,g^{-1}$) in acidic solution[25, 26]. The ratio of Pt-Pd has a great impact on surface morphology and catalytic activity. In the presence of Pd, Pt-Pd/C exhibits larger ECSA, higher mass activity, and larger particle size.

The impact of Pt-Pd/C with different atomic ratios on the particle size, mass activity (MA), and ECSA values are depicted in Figure 2. From the graph, it is clear that smaller particle size is expected for better ORR activities. A relationship is observed between ECSA and the particle size and ratio. Particle size shows an increasing trend with an increasing Pt: Pd in compositions, and ECSA shows a decreasing trend with the increasing Pt: Pd. A higher amount of Pd, i.e. above 1:2 (Pt: Pd), causes a lower dispersion rate, which is the key reason for the decrease in catalytic activity and mass activity [27]. Pd increases overall ORR performance, especially stability in both acidic and alkaline-aqueous electrolytes. A low particle dispersion rate still occurs if the ratio of Pt: Pd is more significant than 1:2. So, it is a major question of which ratio will be taken into consideration.

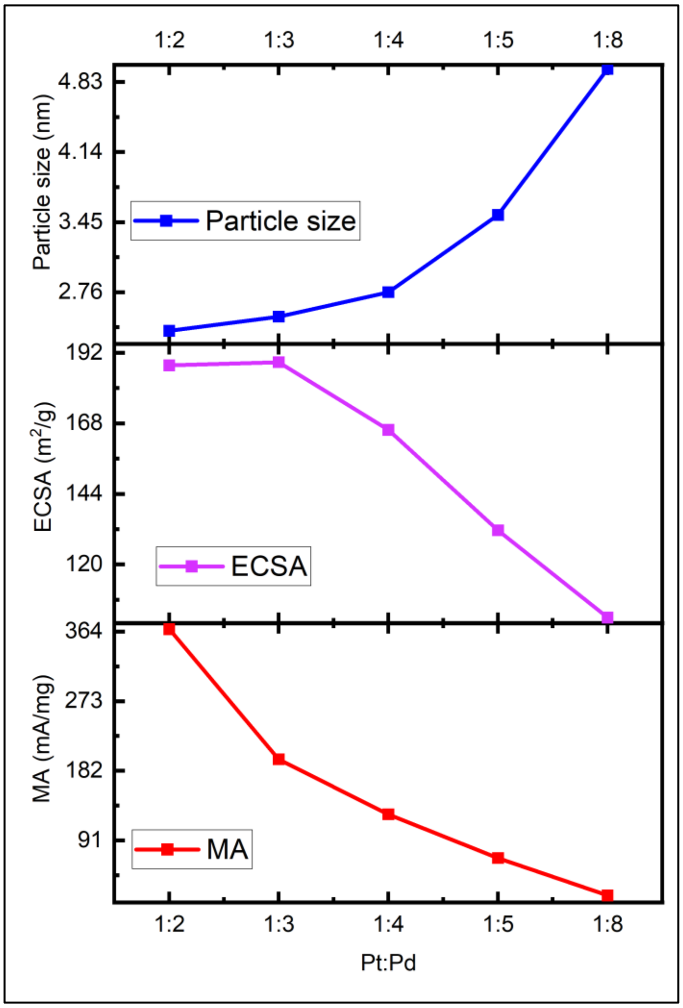

Figure 2. The Impact of Pt: Pd on particle size MA, and ECSA [27]

Ru is another alternative metal for reducing the use of Pt and improving catalytic activity. Small particles show better CO tolerance than large particles for Pt-Ru alloys. The Pt: Ru ratio of 1:1 exhibits an enhanced ORR activity, and the morphological change induces several active sites for CO oxidation, but the oxidation state of Ru is gradually decreased by increasing particle size [28]. In both types of electrolytes. Pt-Ru alloy exhibited better mass activity and stability than state of art Pt/C. Ru surface facilitates the break of O-O bond and supports the proton transport at the same time. As a result, Pt nanoparticles exhibited enhanced ORR catalytic activity [29, 30]. The ECSA, mass activity, and Pt-Ru particle size vary with Pt atom in alloys[31]. According to the literature, the degree of alloying Pt-Ru strongly depends on the nature of the electrolyte. The particle size of the Pt-Ru catalyst decrease with increasing pH of solution[32]. The main drawback of Pt-Ru alloy is that it needs more Pt than Pt-Pd, and as a single metal catalyst, Ru/C exhibits lower catalytic activity compared with Pd/C, Ir/C, and Rh/C in acidic media [33].

In acidic solution, Pt-Pd/C and Pt-Ir/C both catalysts exhibited almost the same ECSA and both catalysts performed better than Pt/C. In terms of stability, Pt-Ir/C was better than Pt-Pd/C and Pt/C. Pt and Ir's nucleation helps to improve the durability and catalytic activity. Crystallite size could be able to tune the performance of Pt-Ir [34, 35]. The mass ratio is the most important factor for the Pt-Ir catalyst. The Pt-Ir/C (16:84) presents a larger ECSA value, which is 28.7 $m^2\ g^{-1}$, and its mass activity is 373.3 mA mg_{pt}^{-1}, which is greater than Pt/C (ECSA=18.3 $m^2\ g^{-1}$ and MA=142.9 mA mg_{pt}^{-1}). However, Pt-Ir/C (4:96) and Pt/C possess the same ECSA value, but Pt-Ir/C (4:96) exhibits lower catalytic activity than Pt/C [36]. Like other Pt group metal alloys, Pt-Ir follows the 4e- pathway and exhibits improved ORR activity. Catalytic performances of this catalyst are strongly influenced by the synthesis technique, treatment temperature, catalyst support, and the presence of Pt [37].

Pt-Rh alloy also exhibits better durability than a single Pt catalyst. Rh itself does not participate in the activity of the catalyst, but the existence of Rh plays a crucial role[38]. Rh covers only 15%–20% of the surface because Pt suppresses it. Both metals possess a similar crystal structure and similar-sized cells. So, it is difficult to determine the active phase that belongs to Rh. A small amount of Rh is needed to make a Pt-Rh alloy and acts as a bimetallic catalyst[39]. Narayanamoorthy et al[40] reported that supportless Pt-Rh alloy is better than Pt-Rh catalyst with Vulcan carbon (VC) and Pt/C (CB). Supportless Pt-Rh (154.4 m^2g^{-1}) possesses a higher ECSA value than Pt-Rh/C (103.5 $m^2\ g^{-1}$) and is 2.5 times higher than Pt-Rh/VC (61.76 $m^2\ g^{-1}$). The cluster morphology depends on the availability of Pt surface[40]. Several studies concluded that smaller particle sizes presented larger ECSA, which exhibit higher mass activity and stability. All PGM alloys follow the $4e^-$ pathway and exhibit comparable catalytic activity in both electrolytes.

Making alloys with low-cost materials is a good strategy for reducing Pt use. TMs are the most acceptable metals for changing the electronic configuration in the cluster [41]. The addition of PGM increases the particle size, whereas Ag reduces the particle size due to its small diameter (<5 nm), facilitating ECSA and ORR activity. Many investigations have been performed on Ag to overcome the limitation of Pt/C [42]. The catalytic activity of Pt-Ag/rGO is slightly higher than that of Pt/C in acidic solution with a Pt: Ag ratio of 1:3.This catalyst exhibits a larger ECSA value (67.8 $m^2\ g^{-1}$) than Pt/C (39.2 $m^2\ g^{-1}$) [43]. Pt-M/C (M=Fe, Co, Ni) presents a larger particle size compared with Pt/C. The particle size of Pt-M/C is calculated to be 2.5 nm to 2.8 nm, whereas that of Pt/C is 2.1 nm when the ratio of Pt: M is 50:50. Pt-Fe/C (100 $m^2\ g^{-1}$) exhibits the highest ECSA value among Pt-M/C, which is lower than 50 wt% of Pt/C (119 $m^2\ g^{-1}$). All Pt-M/C show improved mass activity compared with Pt/C. The variable electron state of TM atoms induces a strong interaction between TM-O, which encourages the slower loss rate of ECSA than PGM [44, 45].

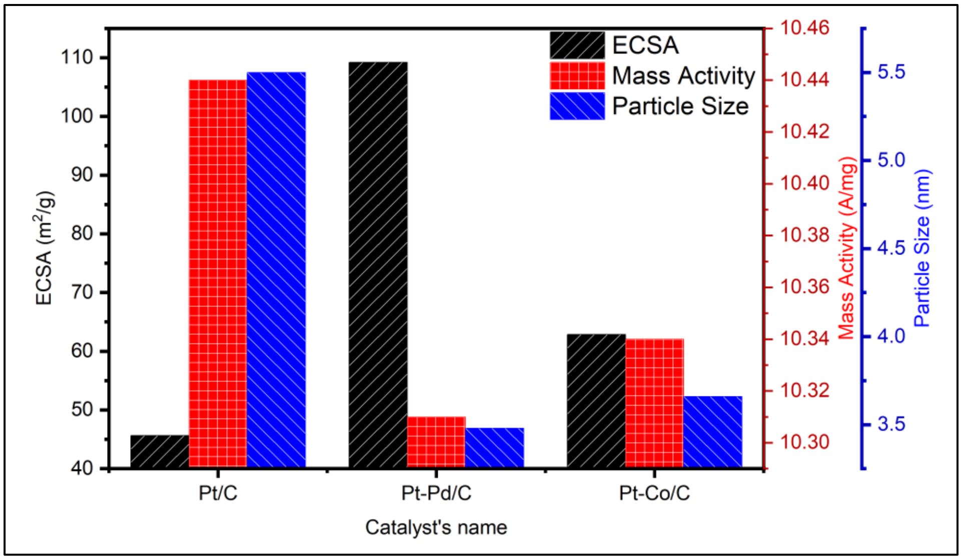

Figure 3. Effect of making alloy with platinum group metal (PGM) and transition metal (TM) [46]

From Figure 3, it has been seen that Pt-Pd/C increases the ECSA and decreases the particle size. On the other hand, Pt-Co/C reduces the ECSA, and particle size was a little larger than Pt-Pd/C. In the case of MA, TM exhibited better performance than PGM. Catalytic activity increased due to lattice compression, resulting from the downward shift of the d-band center of Pt and Pd. ORR activity showed a decreasing trend with an increasing amount of Co. Compare with Pt-Pd/C and Pt/C, Pt-Co/C showed better stability in acidic solution. However, it has been suffering from low stability while using in Toyota Mirai Fuel Cell Vehicles [46–49]. To overcome the stability problem, Pt-Fe/C is a good substitute for Pt/C. Fe can tune the electronic structure of Pt that enhanced the durability of Pt-Fe/C in an acid medium [50, 51]. PGM sites' surface activity has been influenced by the small atomic size of TM and the reduction in the PGM-TM bond, which serves better catalytic activities of PGM-TM alloys. The study revealed that the enhancement of ORR performance depends on the density of PGM [52].

According to literature, the observed improvement in catalytic activity reveals several issues that should be considered in future studies to develop a better catalyst, as follows: (i) increase in the resistance to particle sintering; (ii) surface roughening due to the removal of some alloying metal that increases the electrochemical surface area; and (iii) preferential crystal orientation [52–55]. High durability and catalyst activity are the keys to solving the current problem of Pt. PGM and PGM-TM alloy catalysts exhibit excellent activity and stability compared with traditional Pt/C catalysts. All types of mixed metal alloys are suitable substitutes for commercial Pt/C in alkaline electrolytes. In acidic electrolytes, these catalysts show poor performances without Pt in their composition. PGM-TM bond helps increase durability and stability, but a large amount of PGM is needed to exhibit better catalytic activity.

TM alloy catalysts for ORR

Many experimental studies proved that nitrogen-doped carbon support increases the concentrations of ORR active sites and stability by associating two adjacent carbon crystallites of TM catalyst; the configuration of TM active sites changes completely according to C-N species [56–58]. Here, we discuss some promising TM catalysts that exhibit improved ORR activity in the presence of N.

Fe-N-C has drawn much attention due to its catalytic performances. N coordinated Fe atom has been a highly active center for ORR [59]. Fe-N-C nanoparticles show outstanding stability in both acidic and alkaline solutions. Only 0.5 wt% of the Fe-contained Fe-N-C catalyst possesses a high surface area (1501 m^2g^{-1}) and exhibits superior durability to Pt/C. Half wave potential ($E_{1/2}$) of Fe-N-C and commercial Pt/C is presented in Figure 4.

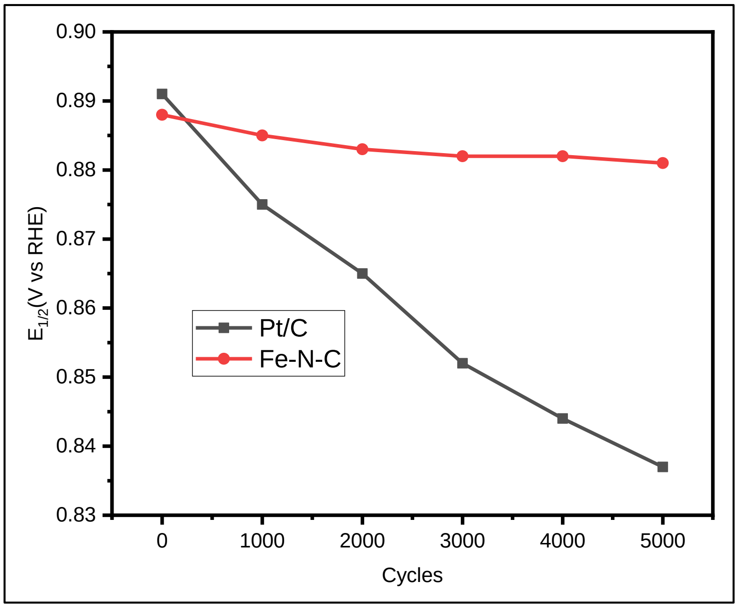

Figure 4. $E_{1/2}$ of Fe-N-C and Pt/C at every 1000 cycles in the durability test [60]

From Figure 4, it is clearly observed that after 5000 potential cycles, Fe-N-C remains unchanged whereas Pt/C gradually decreases under the same condition [60, 61]. The formation of Fe-N is powerfully demonstrated by carbon chemistry. Fe-N active sites are also an essential issue for ORR activity. The Fe-N/C/rGO (10% to 20% of Fe) exhibits improved ECSA and ORR activity, which are comparable with those of Pt/C and are higher in comparison with those of Fe-N/C/rGO (5%–10% of Fe), Fe-N/C, and Fe-N/rGO [62, 63]. Fe-N-based catalyst follows the $4e^-$ reaction pathway in both types of electrolytes. The weight percentage of Fe plays an important role in the composition. This percentage depends on the presence of inducing elements, such as N, P, and S [64]. The gap between the valence and conduction bands of Fe atom (-0.82 eV) enhances catalytic stability and a small amount of metal doping can increase conductivity, and durability [65]. Jiang et al reported that the binding energy of O_2 that presents in the Fe-N_x site helps the adsorption of O_2 on Fe-N_x sites, which promotes ORR activity of Fe-N-C. 20wt% to 35wt% ionomer concentration increases the ionic conductivity of the cathode site. Above 35 wt.% concentration, active sites gradually decrease. However, unsaturated Fe can change the charge density of N-doped carbon support and the central Fe atom in Fe-N_x. Some researchers replaced Fe with Co or Ni [66–68].

Co is the most widely used substitute and partial substitute metal in compositions due to its low price, high durability, and $4e^-$ reaction selectivity [69]. The Co-based catalyst exhibited superior stability to that of Fe. Like Fe, the bimetallic atom-doped Co catalyst shows better ORR performance by forming dual sites than a single metal Co catalyst. Double active sites facilitate electron transfer [70]. Partially substituted Co-Te/C (1:1.93) and Co-Se/C (1:1.25) are catalysts that follow the $4e^-$ reaction pathway in acidic solution, but the catalytic activity is not comparable with that of Pt/C [71]. Support metal has an impact on Co-based catalytic activity. Co_2P/NRC nanorods enhance durability and catalytic action to a level comparable to Pt/C in alkaline media [72]. The performance of the Co-N-C-based catalyst depends on the active site of Co-N_x and nitrogen-containing functional groups and the effect of mutual interaction between Co-O-C and Co-N-C bond formations. Co-N/C catalyst follows the 4e$^-$ reaction pathway and exhibits high durability and current density. High amounts of Co^{2+} oxidation states are associated with increasing ORR activity [41, 57, 73]. Co-Fe alloy is among the prominent non-PGM catalysts for ORR. It has been reported that charge redistribution between Fe-Co alloy and N-supported graphitic carbon-nanotube enhances the catalysts' behavior. The corrosion resistance and electronic conductivity increase with the amount of Co increase in alloy [74, 75].

Ni-based catalyst is another good alternative to most active Pt-group metal catalysts. Ni or Ni alloys are not easily oxidizable, and the Ni structure facilitates the transportation of ions and the charge conductivity[76]. N-doped Ni-Co and Fe-Ni catalysts showed comparable ORR performance with Pt/C and exhibited superior stability [77, 78]. The enhancement of catalytic activity completely depends on the mutual effect of Ni and the N-carbon metal's electronic structures. The edge N atom and the geometric effect of support metal regulate the electronic configuration of Ni [79, 80]. Ni-Mo catalyst showed the highest mass activity among Pt free catalysts used in the present time due to the high dispersion of Ni particles, and Mo facilitates mass activity[81]. In an alkaline aqueous solution, the N-C structure works as a support of the Ni nanoparticles and enhances the catalytic activity towards ORR [79].

As a 3d transition metal, Cu shows high electro-catalytic activity towards ORR due to its valence electron configuration, which is closest to Pt. It has a very strong complex ability to generate Cu-N bonds and exhibits the highest stability in an aqueous solution among 3d transition metals [82]. Cu metal works as an active component for ORR, and this metal is used for constituting active sites. Cu enlarges the surface area of the catalyst. Cu^{2+} ions have a great affinity to form a stable complex with N-based ligands. Cu-N interaction speeds up the peroxide reduction and oxygen activation [83, 84]. The CuFe/C (1.5wt.% Fe and 1.7 wt.% Cu) alloy catalyst and Pt/C (30%) exhibit the same catalytic activity. Fe^{3+}-N works as an active site for ORR, and Cu^{2+}/Cu^{+} plays the role of a redox mediator that shuttles the electron from the electrode to FeN-O$_2$ [85]. During ORR, the Fe atom in Cu alloy facilitates the desorption of oxygenated intermediates, which increases the rate of ORR kinetics. The electronic structure of catalyst metals has been changed by the interaction between the metal catalyst and the support metal. N particularly helps donate electrons to the O-O bond, thereby increasing stability [86]. Cu ascribes to high redox potentials, and the current densities of the d-orbital of Cu lead to a weaker O-O bond [87].

Among the transition metals, manganese oxides became the focus of research due to their variable oxidation states and high stability in alkaline media. Mn^{3+} species modifies the crystallinity, surface area, and pore size of catalysts [88]. Liu and co-workers identified the two types of Mn coordination, octahedral Mn^{4+} (i.e. partial d-orbital filling Mn) and pyramidal Mn^{3+} and Mn^{3+} coordination is essential for ORR activity [89]. The N-C structure helps reduce electron cloud densities on a carbon atom by inducing N. The active site of the Mn-N-C catalyst is the combined structure of N-C and Mn-N [90]. The covalency of the Mn-O bond is responsible for specific ORR activity and works as an electron transfer mediator to O. The existence of Mn^{3+} on the active site facilitates the ORR activity, whereas Mn^{4+} encourages the 4e$^-$ reaction pathway [91].

However, TM based catalysts exhibit higher levels of ORR activity in alkaline media that indicate the exchange of electrons and the change of oxidation state during ORR, the exact role of TM is not clear[57]. Transition metals (TM) have been recognized as alternatives due to their high corrosion resistance and stabilities, electrical conductivities, and mechanical strengths. N-doped carbon-supported TM catalyst exhibits better ORR activity in alkaline solution. Formation of C-N increases the concentration of active sites.

Benefits of the carbon support

Carbon support helps increase the electronic behavior of catalysts and enhances ORR performance. ECSA, durability, reaction pathway, and electrical conductivity have been influenced by support materials [92]. Corrosion of metal is an important factor in fuel cell operations. Carbon support metal helps overcome corrosion problems by making a strong bond between nanoparticles and support materials [93]. Carbon nanomaterials are considered good catalyst support due to their excellent properties, which ensure the following parameters: 1) high electrical conductivity; 2) large surface area; 3) strong interaction between support and catalyst; 4) high electrical stability under the fuel cell condition, and 5) low cost [94–96]. Large surface areas of support suppress the particle size. This criterion helps make a highly concentrated catalyst particle that increases the efficiency of the electrode by reducing embedded sites and shortening the reactant pathway [97, 98]. C(Carbon black) is widely used for commercial Pt catalysts. Poor durability and low catalyst metal utilization are the main weaknesses of C. GO (graphene oxide), rGO (reduced graphene oxide, MWCNT(multiwall carbon nanotube), and so on are considered a better substitute for C. [99, 100]. Nowadays, GO and rGO are widely used because of the partial transition from sp^2 to sp^3carbon atoms. Both GO and rGO derivatives of graphene are easy to produce on a large scale using graphene sheets, catalyst metal is located between pores, thereby reducing the aggregation of catalyst metals, and this behavior helps enhance catalyst efficiency [101, 102]. Studies revealed that in rGO, oxygen groups participate in the transfer of electrons, which causes the reduction of catalytic activity. Electric contact efficiency plays an important role between two catalyst particles. rGO has higher thermal stability than GO due to lower defect density [103, 104].

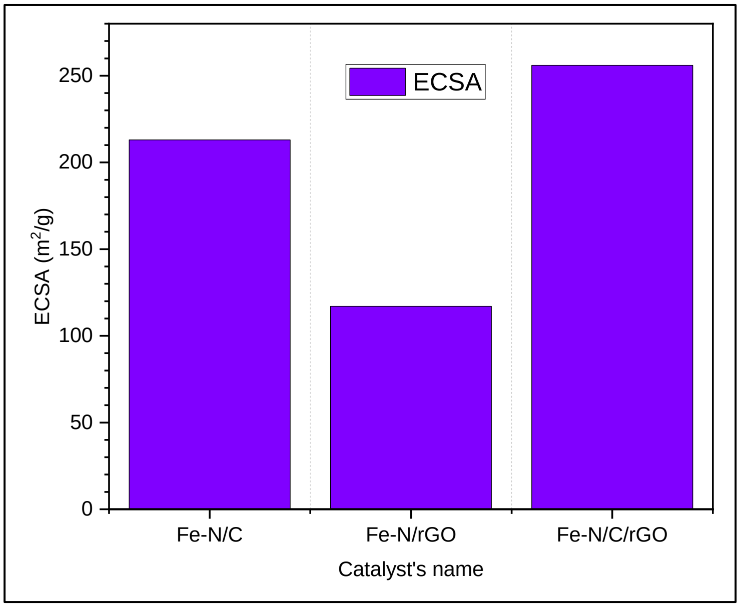

Figure 5. Effect of carbon support on ECSA [63]

It has been seen from Figure 5, ECSA of catalysts changes with the change of support metal, carbon black (C) supported Fe catalyst exhibited larger ECSA than reduced graphene oxide (rGO). Fe catalyst presented the largest ECSA while C and rGO were used together [63] Surface modification of the graphene sheet is conducted by inducing the heteroatom to boost the interaction with a metal catalyst; graphene aggregation is avoided by changing the interfacial properties [105]. The electrochemical activity of the non-PGM catalyst depends on the doped element (N, S, and P) that supports carbon. The edge plane sites contribute to the improvement of catalytic performances, and spin densities on adjoining carbon atoms induce different ORR sites [64, 106–109]. Based on the above discussion, we summarise the properties of different carbon forms in Table 1, that influence the ORR activity.

Table 1. Represents the ECSA, conductivity, advantages, and disadvantages of widely used carbon forms as support

Carbon Materials	**ECSA ($m^2 g^{-1}$)**	**Conductivity ($S\ cm^{-1}$)**	**Advantages**	**Disadvantages**	**Ref.**
Vulcan XC-72	250	2.77	The catalytic activity can be increased by surface modification and pre-heat treatment.	Low utilization of metal catalysts and poor durability.	[110, 111]
CNT	50-1000	200-900	Excellent electrochemical stability and high hydrophilicity produce better ORR reactions.	Highly sensitive to different gas and synthesis methods.	[52, 112, 113]
GO	2630	$\sim 10^4$	Easy to synthesis on an industrial scale and functionalized as well.	Catalytic properties change with changing synthesis tech.	[114–116]
Ordered porous carbon(OPC)	600-2800	$3.28 x 10^{-4}$ - $2.2 x 10^{-3}$	Stability increases with increasing annealing temperature	Electrochemical activities strongly depend on pore size and the diameter less than 10nm.	[117–120]
Graphene nanosheets (GNS)	56	10^3-10^4	Highly stable than MWCNT, SWCNT, CB, and GO	Highly sensitive to the synthesis process. During preparation, it losses many properties due to aggregate.	[98, 121, 122]

Promising synthesis technique for ORR catalysts

The synthesis condition influences the catalyst compositions and structure of active sites. Several strategies are used to establish a catalyst that is comparable to Pt/C in both acid and base solutions. Among the improvement techniques, pyrolysis and core-shell techniques are widely used for developing alloy catalysts. Most recently, the irradiation method utilizes for obtaining a higher degree of alloying.

Pyrolysis

Different types of metal alloys help reduce PGM use and help modify the surface structure and reactivity within alloying elements through the change of electronic and geometric structure [11, 111]. Alloying PGM with transition metals declines the OH adsorption due to the existence of PGM-TM bond distance in lattice contraction, which promotes higher ORR activity than pure PGM. The durability of PGM-TM alloys depends on the degree of alloy homogeneity [52, 123]. Performances of alloy catalysts are directly related to pyrolysis treatment. The effect of pyrolysis temperature has been illustrated in Figure 6(a-f).

From the TEM image of FeCN/GN(graphene nanosheets), it is clear that below 700° C, only a few FeCN particles have been observed, marked by the white circle in Figure 6(a) and 6(b) which were pyrolyzed at 500° C and 600° C respectively. Figure 6(d-f) represents FeCN samples that pyrolyzed at 800 °C, 900 °C, and 1000 °C respectively. FeCN particles were uniformly distributed on GN(graphene nanosheets) above 700 °C. Figure 6(c) represents the sample pyrolyzed at 700 °C. At 700 °C, FeCN/GN exhibited the highest electron transfer (3.94) and ORR activity in acidic solutions. In general, a pyrolysis temperature below 700 °C is not enough to induce stable and active ORR sites [112, 124, 125]. The formation of Fe-N_x active sites strongly depends on pyrolysis, which contributes to ORR activity. N atoms have been successfully united into a carbon matrix, and the proportion of N touches the maximum level at 900 °C [53,119]. The pyrolysis treatment approach helps increase the concentration of ORR sites by modifying the M-N_x/C structure. Heat treatment also controls metal-N bonding [76,120].

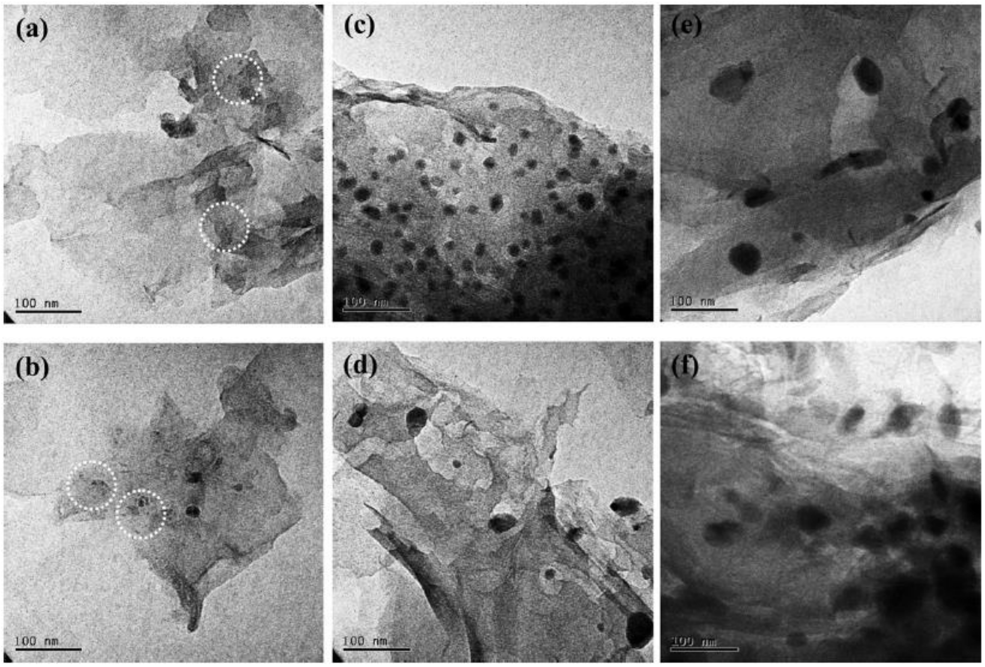

Figure 6. TEM image of FeCN/GN at 500 °C (a), 600 °C (b), 700 °C (c),800 °C (d), 900 °C (e), and 1000 °C (f) [124]

Core-shell structure

Mutual interaction of core metal and shell facilitates the mass activity and durability of ORR in both acidic and alkaline electrolytes. Generally, a core-shell-structured catalyst is designed by capturing the catalyst metal in carbon materials. This structure provides an exclusive electronic interaction between confined nanomaterials and carbon shells, thereby playing the main role in the enhancement of catalytic activity. Both single metal particles and metal alloy materials can serve as shells or core [105, 108]. This approach leads to a change in the d-band positions, which help provide higher activation energies. Ligand performances enhance catalytic activity and improve charge transfer [100]. Core materials and shell thickness are important factors for stability and ORR performance. Shell thickness helps with long term stability. The thickness of the shell screens the core interactivity, which improves catalytic stability [31, 115]. Gautam et al. reported that a shell material graphene nanosheets appears on behalf of electron collectors and tricks the core ion to form the existing active sites by providing high stability [116]. [116]

Irradiation technique

The irradiation process helps improve structural properties and chemical properties. γ-Irradiation helps reduce the oxygen functional group from the GO sheet and increases C=C bands. It also modifies the sp^2 character of C. Some work has been done using gamma irradiation. In the case of few-layered graphene materials, the O/C ratio exhibits a decreasing trend when γ-irradiation dose increases for GO and GONR (nanorod) [117]. A remarkable characteristic has been observed in preparing graphene aerogel (GA) from the GO sheet. GA shows more stability and has a honeycomb structure with a high C/O ratio after irradiation. No significant weight loss can be observed due to γ-irradiation.[118]. However, dose rate, total dose, type of solvent are important parameters for gamma irradiation induced synthesis technique. These parameters can be able to alter the size, chemical, and physical properties of the final product. Sharin and co-workers reported the reduction of GO has occurred when the cumulative dose was 35kGy. They utilized different amounts of irradiation dose,0, 5, 15, 20, and 35kGy on GO powders [119, 126, 127] In an aqueous solution (water/alcohol), Irradiation decompose the water molecules to hydroxyl radical, OH^-, hydrogen radical, and hydrated electron, H^* and e^- species. Alcohol removes the oxidative OH and converts it into reductive radicals.[121]. In the case of a heterogeneous catalyst, gamma irradiation changes the concentration of the active site of a catalyst surface, whereas electron beam irradiation induces a new active center by switching the chemical bond and creating defects on a catalyst surface [128]. Kakitani et al. reported that Pt-C bond formed during ion-beam irradiation (Ar^+). This bond changes the chemical state of Pt nanoparticles and carbon support that suppresses Pt oxidation and improves overall catalytic activity towards ORR [129]. After Ar^+ irradiation, carbon nanofiber-supported PtRu exhibits a lower crystal size (19.5 nm) due to the change in the valence state of support metal, whereas non-irradiated carbon nanofiber-supported PtRu shows a larger crystal size (20.1 nm) [130]. Proton irradiation leads to a break M (metal)-O bond by producing highly active radicals on the metal surface. During irradiation, the 2p orbital of O and the 3d orbital of metal merge, thereby reducing the bang gap, which increases the electronic conductivity and overall performance of the metal catalyst [131]. Ohkubo and co-workers suggested that the electron beam irradiation reduction method can synthesize both alloy and metal oxide on the carbon support simultaneously[132].

Conclusion

From the discussions, it is clear that all PGM alloys are comparable catalysts for ORR cathode in both acid and alkaline mediums, though 20%wt of Pt is needed for promising performance. Mixing PGM and transition metal is a good strategy for reducing the use of Pt. PGM-TM alloy catalysts also improve ORR activity and follow the $4e^-$ pathway in both types of solutions. However, 50wt% of PGM is required in the PGM-TM cluster for enhancing ORR activity. Most of the TM-based catalysts have been developed with the N supported carbon. N atom produces C-N sites that provide higher active site densities and mass transport. In the absence of the N atom, the TM-based catalysts are not comparable with commercial Pt/C and other PGM catalysts. N supported Fe, and Fe doped Co catalysts work in acidic solutions, but it is not comparable with commercial Pt/C. All M-N-C (M= transition metal) exhibited better catalytic activity than Pt/C in alkaline solution. Choosing ideal carbon support can improve the catalytic activity of TM alloy in an acidic medium. The amount of nitrogen and carbon defects and metallic particles' existence are common factors for improving performance.

Alloy and pyrolysis are closely related to each other. Homogeneity of alloy catalysts depends on pyrolysis temperature. Core-shell is a popular technique for alloy catalysts. In this process, catalyst behaviour is associated with the mutual interaction between the core metal and the shell metal. Shell thickness also plays a hidden role to facilitates ORR. Nowadays, different types of irradiations have been taken a superior position in research.

Acknowledgment

This paper was completed with the financial assistance of Universiti Kebangsaan Malaysia (GUP-2018-041) and the International Atomic Energy Agency (R23130) and support of Fuel Cell Institute, UKM.

References

1. Rajapakse, R. M. G., Senarathna, K. G. C., Kondo, A., Jayawardena, P. S. and Shimomura, M. (2015). Extremely low-cost alternative for the oxygen reduction catalyst of fuel cell. *Advances in Automobile Engineering,* 4(1): 1.
2. Zhang, Y., Huang, N., Zhou, F., He, Q. and Zhan, S. (2018). Research on the oxygen reduction reaction (ORR) mechanism of g-C_3N_4 doped by Ag based on first-principles calculations. *Journal of the Chinese Chemical Society*, 65(12): 1431-1436.
3. She, Y., Chen, J., Zhang, C., Lu, Z., Ni, M., Sit, P. H. L. and Leung, M. K. H. (2017). Oxygen Reduction reaction mechanism of nitrogen-doped graphene derived from ionic liquid. *Energy Procedia*, 142: 1319-1326.
4. Hazarika, K. K., Goswami, C., Saikia, H., Borah, B. J. and Bharali, P. (2018). Cubic Mn_2O_3 nanoparticles on carbon as bifunctional electrocatalyst for oxygen reduction and oxygen evolution reactions. *Molecular Catalysis,* 451: 153-160.
5. Laurent-Brocq, M., Job, N., Eskenazi, D. and Pireaux, J. J. (2014). Pt/C catalyst for PEM fuel cells: Control of Pt nanoparticles characteristics through a novel plasma deposition method. *Applied Catalysis B: Environmental*, 147: 453-463.
6. Shao-Horn, Y., Sheng, W. C., Chen, S., Ferreira, P. J., Holby, E. F. and Morgan, D. (2007). Instability of supported platinum nanoparticles in low-temperature fuel cells. *Topics in Catalysis*, 46(3–4): 285–305.
7. Dombrovskis, J. K. and Palmqvist, A. E. C. (2016). Recent progress in synthesis, characterization and evaluation of non-precious metal catalysts for the oxygen reduction reaction. *Fuel Cells*, 16(1): 4-22.
8. Holton, O. and Stevenson, J. (2013). The role of platinum in proton exchange membrane fuel cells - Johnson Matthey technology review. *Platinum Metals Reviews*, 57(4): 259-271.
9. Mustain, W. E., Shrestha, S., Ashegi, S., Timbro, J., Lang, C. M. and Mustain, W. E. (2011). ORR and fuel cell performance of Pt supported on N-functionalized mesoporous carbon, *ECS Transactions*, 41(1): 1183.
10. Ghosh, S., Mondal, S. and Retna Raj, C. (2014). Carbon nanotube-supported dendritic Pt-on-Pd nanostructures: Growth mechanism and electrocatalytic activity towards oxygen reduction reaction. *Journal of Materials Chemistry A*, 2(7): 2233-2239.
11. Guha, A., Lu, W., Zawodzinski, T. A. and Schiraldi, D. A. (2007). Surface-modified carbons as platinum catalyst support for PEM fuel cells, *Carbon,* 45: 1506-1517.
12. Mun, Y., Lee, S., Kim, K., Kim, S., Lee, S., Han, J. W. and Lee, J. (2019). Versatile strategy for tuning ORR activity of a single Fe-N4 site by controlling electron-withdrawing/donating properties of a carbon plane. *Journal of the American Chemical Society*, 141(15): 6254-6262.
13. Kodali, M., Santoro, C., Serov, A., Kabir, S., Artyushkova, K., Matanovic, I. and Atanassov, P. (2017). Air breathing cathodes for microbial fuel cell using Mn-, Fe-, Co- and Ni-containing platinum group metal-free catalysts. *Electrochimica Acta*, 231: 115-124.

14. Song, M., Song, Y., Sha, W., Xu, B., Guo, J. and Wu, Y. (2020). Recent advances in non-precious transition metal/nitrogen-doped carbon for oxygen reduction electrocatalyst. *Catalysts*, 10(1): 141.
15. Mao, J., Liu, P., Du, C., Liang, D., Yan, J. and Song, W. (2019). Tailoring 2D MoS_2 heterointerfaces for promising oxygen reduction reaction electrocatalysis. *Journal of Materials Chemistry A*, 7(15): 8785-8789.
16. Ma, R., Lin, G., Zhou, Y., Liu, Q., Zhang, T., Shan, G. and Wang, J. (2019). A review of oxygen reduction mechanisms for metal-free carbon-based electrocatalysts. *NPJ Computational Materials*, *5*(1): 1-15.
17. Tang, Z., Wu, W. and Wang, K. (2018). Oxygen reduction reaction catalyzed by noble metal clusters. *Catalysts*, 8(2): 65.
18. Kim, J. Y., Oh, T. K., Shin, Y., Bonnett, J. and Weil, K. S. (2011). A novel non-platinum group electrocatalyst for PEM fuel cell application. *International Journal of Hydrogen Energy*, 36(7): 4557-4564.
19. Wang, B. (2005). Recent development of non-platinum catalysts for oxygen reduction reaction. *Journal of Power Sources*, 152(1–2): 1-15.
20. Sui, S., Wang, X., Zhou, X., Su, Y., Riffat, S. and Liu, C. J. (2017). A comprehensive review of Pt electrocatalysts for the oxygen reduction reaction: Nanostructure, activity, mechanism and carbon support in PEM fuel cells. *Journal of Materials Chemistry A*, 5(5): 1808-1825.
21. Raciti, D., Kubal, J., Ma, C., Barclay, M., Gonzalez, M., Chi, M. and Wang, C. (2016). Pt_3Re alloy nanoparticles as electrocatalysts for the oxygen reduction reaction. *Nano Energy*, 20: 202-211.
22. Hyun, K., Lee, J. H., Yoon, C. W. and Kwon, Y. (2013). The effect of platinum based bimetallic electrocatalysts on oxygen reduction reaction of proton exchange membrane fuel cells. *International Journal of Electrochemical Science*, 8(10): 11752-11767.
23. Tian, J., Wu, W., Tang, Z., Wu, Y., Burns, R., Tichnell, B. and Chen, S. (2018). Oxygen reduction reaction and hydrogen evolution reaction catalyzed by Pd–Ru nanoparticles encapsulated in porous carbon nanosheets. *Catalysts*, 8(8): 1-15.
24. Zhou, Z. M., Shao, Z. G., Qin, X. P., Chen, X. G., Wei, Z. D. and Yi, B. L. (2010). Durability study of Pt-Pd/C as PEMFC cathode catalyst. *International Journal of Hydrogen Energy*, 35(4): 1719-1726.
25. Wang, W., Wang, Z., Wang, J., Zhong, C. J. and Liu, C. J. (2017). Highly active and stable Pt–Pd Alloy catalysts synthesized by room-temperature electron reduction for oxygen reduction reaction. *Advanced Science*, 4(4): 1-9.
26. Yusof, M. S. M., Jalil, A. A., Ahmad, A., Triwahyono, S., Othman, M. H. D., Abdullah, T. A. T. and Nabgan, W. (2019). Effect of Pt–Pd/C coupled catalyst loading and polybenzimidazole ionomer binder on oxygen reduction reaction in high-temperature PEMFC. *International Journal of Hydrogen Energy*, 2019: 20760-20769.
27. Thanasilp, S. and Hunsom, M. (2011). Effect of Pt: Pd atomic ratio in Pt-Pd/C electrocatalyst-coated membrane on the electrocatalytic activity of ORR in PEM fuel cells. *Renewable Energy*, 36(6): 1795-1801.
28. Jackson, C., Conrad, O. and Levecque, P. (2017). Systematic study of Pt-Ru/C catalysts prepared by chemical deposition for direct methanol fuel cells. *Electrocatalysis*, 8(3): 224-234.
29. Huang, H., Zhu, J., Li, D., Shen, C., Li, M., Zhang, X. and Wu, Y. (2017). Pt nanoparticles grown on 3D RuO_2-modified graphene architectures for highly efficient methanol oxidation. *Journal of Materials Chemistry A*, 5(9): 4560-4567.
30. Yang, G., Sun, Y., Lv, P., Zhen, F., Cao, X., Chen, X. and Kong, X. (2016). Preparation of Pt–Ru/C as an oxygen-reduction electrocatalyst in microbial fuel cells for wastewater treatment. *Catalysts*, 6(10): 150.
31. Jackson, A., Strickler, A., Higgins, D. and Jaramillo, T. F. (2018). Engineering Ru@Pt core-shell catalysts for enhanced electrochemical oxygen reduction mass activity and stability. *Nanomaterials*, *8*(1): 38.
32. Tolmachev, Y. V. and Petrii, O. A. (2017). Pt–Ru electrocatalysts for fuel cells: developments in the last decade. *Journal of Solid State Electrochemistry*, 21(3): 613-639.

33. Durst, J., Simon, C., Hasché, F. and Gasteiger, H. A. (2015). Hydrogen oxidation and evolution reaction kinetics on carbon supported Pt, Ir, Rh, and Pd electrocatalysts in acidic media. *Journal of The Electrochemical Society*, 162(1): F190-F203.
34. Zeng, M., Wang, X. X., Tan, Z. H., Huang, X. X. and Wang, J. N. (2014). Remarkable durability of Pt-Ir alloy catalysts supported on graphitic carbon nanocages. *Journal of Power Sources*, 264: 272-281.
35. Zheng, H. B., An, L., Zheng, Y., Qu, C., Fang, Y., Liu, Q. and Dang, D. (2018). Tuning the catalytic activity of Ir@Pt nanoparticles through controlling ir core size on cathode performance for PEM fuel cell application. *Frontiers in Chemistry*, *6*(7): 1-7.
36. Fang, D., Tang, X., Yang, L., Xu, D., Zhang, H., Sun, S. and Yi, B. (2019). Facile synthesis of Pt-decorated Ir black as a bifunctional oxygen catalyst for oxygen reduction and evolution reactions. *Nanoscale*, 11(18): 9091-9102.
37. Zhu, J., Elnabawy, A. O., Lyu, Z., Xie, M., Murray, E. A., Chen, Z., Xia, Y. (2019). Facet-controlled Pt–Ir nanocrystals with substantially enhanced activity and durability towards oxygen reduction. *Materials Today*, 2019: 1-9.
38. Lin, C., Wu, G., Li, H., Geng, Y., Xie, G., Yang, J. and Jin, J. (2017). Rh nanoparticles supported on ultrathin carbon nanosheets for high-performance oxygen reduction reaction and catalytic hydrogenation. *Nanoscale*, 9(5): 1834-1839.
39. Paál, Z., Gyorffy, N., Wootsch, A., Tóth, L., Bakos, I., Szabó, S. and Schlögl, R. (2007). Preparation, physical characterization and catalytic properties of unsupported Pt-Rh catalyst. *Journal of Catalysis*, *250*(2): 254-263.
40. Narayanamoorthy, B., Datta, K. K. R., Eswaramoorthy, M. and Balaji, S. (2014). Self-stabilized Pt–Rh bimetallic nanoclusters as durable electrocatalysts for dioxygen reduction in PEM fuel cells. *RSC Advances*, 4(98): 55571-55579.
41. Goswami, C., Hazarika, K. K. and Bharali, P. (2018). Transition metal oxide nanocatalysts for oxygen reduction reaction. *Materials Science for Energy Technologies*, 1(2): 117–128.
42. Xin, L., Zhang, Z., Wang, Z., Qi, J. and Li, W. (2013). Carbon supported Ag nanoparticles as high performance cathode catalyst for H_2/O_2 anion exchange membrane fuel cell. *Frontiers in Chemistry*, 1: 16.
43. Esfandiari, A., Kazemeini, M. and Bastani, D. (2016). Synthesis, characterization and performance determination of an Ag@Pt/C electrocatalyst for the ORR in a PEM fuel cell. *International Journal of Hydrogen Energy*, 41(45): 20720-20730.
44. Chiwata, M., Yano, H., Ogawa, S., Watanabe, M., Iiyama, A. and Uchida, H. (2016). Oxygen reduction reaction activity of carbon-supported Pt-Fe, Pt-Co, and Pt-Ni alloys with stabilized Pt-skin layers. *Electrochemistry*, *84*(3), 133–137.
45. Li, W., Pan, Z., Huang, Z., Zhou, Q., Xu, Y., Wu, S., Hu, G. (2018). Pt nanoparticles supported on titanium iron nitride nanotubes prepared as a superior electrocatalysts for methanol electrooxidation. *International Journal of Hydrogen Energy*, 43(20): 9777-9786.
46. Termpornvithit, C., Chewasatn, N. and Hunsom, M. (2012). Stability of Pt-Co/C and Pt-Pd/C based oxygen reduction reaction electrocatalysts prepared at a low temperature by a combined impregnation and seeding process in PEM fuel cells. *Journal of Applied Electrochemistry*, 42(3): 169-178.
47. Cui, Y., Wu, Y., Wang, Z., Yao, X., Wei, Y., Kang, Y., Gan, L. (2020). Mitigating metal dissolution and redeposition of Pt-Co catalysts in PEM fuel cells: Impacts of structural ordering and particle size. *Journal of The Electrochemical Society*, 167(6): 064520.
48. Rohendi, D., Rachmat, A. and Syarif, N. (2018). Fabrication and characterization of Pt-Co/C catalyst for fuel cell electrode. *Journal of Physics: Conference Series*, 1095(1): 012007.
49. Singh, R. N. (2012). Preparation of bimetallic Pd-Co nanoparticles on graphene support for use as methanol tolerant oxygen reduction electrocatalysts. *Engineering, Technology & Applied Science Research*, *2*(6): 295-301.
50. Ramli, Z. A. C. and Kamarudin, S. K. (2018). Platinum-based catalysts on various carbon supports and conducting polymers for direct methanol fuel cell applications: a review. *Nanoscale Research Letters*, 13: 1-25.

51. Mechler, A. K., Sahraie, N. R., Armel, V., Zitolo, A., Sougrati, M. T., Schwämmlein, J. N. and Jaouen, F. (2018). Stabilization of iron-based fuel cell catalysts by non-catalytic platinum. *Journal of The Electrochemical Society*, 165(13): F1084–F1091.
52. Mohanraju, K. and Cindrella, L. (2014). Impact of alloying and lattice strain on ORR activity of Pt and Pd based ternary alloys with Fe and Co for proton exchange membrane fuel cell applications. *RSC Advances*, 4(23): 11939-11947.
53. Li, X. P., Xiang, X. D., Yang, H. Y., Wang, X. J., Tan, C. L. and Li, W. S. (2013). Hydrogen tungsten bronze-supported platinum as electrocatalyst for methanol oxidation. *Fuel Cells*, 13(2): 314-318.
54. Seselj, N., Engelbrekt, C. and Zhang, J. (2015). Graphene-supported platinum catalysts for fuel cells. *Science Bulletin*, 60(9): 864-876.
55. Lv, H., Li, D., Strmcnik, D., Paulikas, A. P., Markovic, N. M. and Stamenkovic, V. R. (2016). Recent advances in the design of tailored nanomaterials for efficient oxygen reduction reaction. *Nano Energy*, 29: 149-165.
56. Thippani, T., Mandal, S., Wang, G., Ramani, V. K. and Kothandaraman, R. (2016). Probing oxygen reduction and oxygen evolution reactions on bifunctional non-precious metal catalysts for metal-air batteries. *RSC Advances*, 6(75): 71122-71133.
57. Osgood, H., Devaguptapu, S. V., Xu, H., Cho, J. and Wu, G. (2016). Transition metal (Fe, Co, Ni, and Mn) oxides for oxygen reduction and evolution bifunctional catalysts in alkaline media. *Nano Today*, 11(5): 601-625.
58. Akbari, A., Amini, M., Tarassoli, A., Eftekhari-Sis, B., Ghasemian, N. and Jabbari, E. (2018). Transition metal oxide nanoparticles as efficient catalysts in oxidation reactions. *Nano-Structures and Nano-Objects*, 14: 19-48.
59. Ren, G., Gao, L., Teng, C., Li, Y., Yang, H., Shui, J. and Dai, L. (2018). Ancient Chemistry “pharaoh’s Snakes” for Efficient Fe-/N-Doped Carbon Electrocatalysts. *ACS Applied Materials and Interfaces*, 10(13): 10778–10785.
60. Gu, L., Jiang, L., Li, X., Jin, J., Wang, J. and Sun, G. (2016). A Fe-N-C catalyst with highly dispersed iron in carbon for oxygen reduction reaction and its application in direct methanol fuel cells. *Cuihua Xuebao/Chinese Journal of Catalysis*, 37(4): 539-548.
61. Park, M., Lee, J., Hembram, K., Lee, K.-R., Han, S., Yoon, C. and Kim, J. (2016). Oxygen reduction electrocatalysts based on coupled iron nitride nanoparticles with nitrogen-doped carbon. *Catalysts*, 6(6): 86.
62. Rahman, K. R., Kok, K. Y., Wong, W. Y., Yang, H. and Lim, K. L. (2021). Effect of iron loading on the catalytic activity of Fe/N-doped reduced graphene oxide catalysts via irradiation. *Applied Sciences (Switzerland)*, 11(1): 1-10.
63. Xi, J., Wang, F., Mei, R., Gong, Z., Fan, X., Yang, H. and Luo, Z. (2016). Catalytic performance of a pyrolyzed graphene supported Fe-N-C composite and its application for acid direct methanol fuel cells. *RSC Advances*, 6(93): 90797-90805.
64. Meng, H., Chen, X., Gong, T., Liu, H., Liu, Y., Li, H. and Zhang, Y. (2019). N, P, S/Fe-codoped carbon derived from feculae bombycis as an efficient electrocatalyst for oxygen reduction reaction. *ChemCatChem*, 11(24): 6015-6021.
65. Basri, S. and Kamarudin, S. K. (2018). Nanocatalyst FeN_4/C molecular orbital behaviour for oxygen reduction reaction (ORR) in cathode direct methano fuel cell (DMFC). *Jurnal Kejuruteraan*, 1(2): 59-64.
66. Jiang, W. J., Gu, L., Li, L., Zhang, Y., Zhang, X., Zhang, L. J. and Wan, L. J. (2016). Understanding the high activity of Fe-N-C electrocatalysts in oxygen reduction: Fe/Fe_3C nanoparticles boost the activity of Fe-Nx. *Journal of the American Chemical Society*, 138(10): 3570-3578.
67. Hossen, M. M., Artyushkova, K., Atanassov, P. and Serov, A. (2018). Synthesis and characterization of high performing Fe-N-C catalyst for oxygen reduction reaction (ORR) in alkaline exchange membrane fuel cells. *Journal of Power Sources*, 375: 214-221.
68. Zhan, Y., Xie, F., Zhang, H., Lin, Z., Huang, J., Zhang, W. and Meng, H. (2018). Non noble metal catalyst for oxygen reduction reaction and its characterization by simulated fuel cell test. *Journal of The Electrochemical Society*, 165(15): J3008-J3015.

69. Kim, S., Park, H. and Li, O. L. (2020). Cobalt nanoparticles on plasma-controlled nitrogen-doped carbon as high-performance ORR electrocatalyst for primary Zn-Air battery. *Nanomaterials*, 10(2): 223.
70. Zang, J., Wang, F., Cheng, Q., Wang, G., Ma, L., Chen, C. and Yang, H. (2020). Cobalt/zinc dual-sites coordinated with nitrogen in nanofibers enabling efficient and durable oxygen reduction reaction in acidic fuel cells. *Journal of Materials Chemistry A*, 8(7): 3686-3691.
71. Grinberg, V. A., Mayorova, N. A., Pasynskii, A. A., Modestov, A. D., Shiryaev, A. A., Vysotskii, V. V. and Nogai, A. S. (2018). Nanostructured platinum-free catalysts of oxygen reduction based on metal chalcogenide cobalt clusters. *Russian Journal of Coordination Chemistry*, 44(10): 589-595.
72. Winey, K. I., Li, J., Doan-Nguyen, V. V. T., Murray, C. B., Su, D., Trigg, E. B. and Agarwal, R. (2015). Synthesis and X-ray characterization of cobalt phosphide (Co_2P) nanorods for the oxygen reduction reaction. *ACS Nano*, 9(8): 8108-8115.
73. Zhao, H., Xing, T., Li, L., Geng, X., Guo, K., Sun, C. and An, B. (2019). Synthesis of cobalt and nitrogen co-doped carbon nanotubes and its ORR activity as the catalyst used in hydrogen fuel cells. *International Journal of Hydrogen Energy*, 44(46): 25180-25187.
74. Liang, G., Huang, J., Li, J., Wu, Y., Huang, G., Jin, Y. Q., ... and Meng, H. (2020). Improving the catalytic performance of Co/N/C catalyst for oxygen reduction reaction by alloying with Fe. J*ournal of The Electrochemical Society,* 167(10), 104502.
75. An, L., Jiang, N., Li, B., Hua, S., Fu, Y., Liu, J. and Sun, Z. (2018). A highly active and durable iron/cobalt alloy catalyst encapsulated in N-doped graphitic carbon nanotubes for oxygen reduction reaction by a nanofibrous dicyandiamide template. *Journal of Materials Chemistry A*, 6(14): 5962-5970.
76. Liu, P., Ran, J., Xia, B., Xi, S., Gao, D. and Wang, J. (2020). Bifunctional oxygen electrocatalyst of mesoporous Ni/NiO nanosheets for flexible rechargeable Zn–Air batteries. *Nano-Micro Letters*, *12*(1), 1–12.
77. Hao, Y., Xu, Y., Liu, J. and Sun, X. (2017). Nickel-cobalt oxides supported on Co/N decorated graphene as an excellent bifunctional oxygen catalyst. *Journal of Materials Chemistry A*, 5(11): 5594-5600.
78. Trzešniewski, B. J., Diaz-Morales, O., Vermaas, D. A., Longo, A., Bras, W., Koper, M. T. M. and Smith, W. A. (2015). In situ observation of active oxygen species in Fe-containing Ni-based oxygen evolution catalysts: The effect of pH on electrochemical activity. *Journal of the American Chemical Society*, 137(48): 15112-15121.
79. Zhuang, Z., Giles, S. A., Zheng, J., Jenness, G. R., Caratzoulas, S., Vlachos, D. G. and Yan, Y. (2016). Nickel supported on nitrogen-doped carbon nanotubes as hydrogen oxidation reaction catalyst in alkaline electrolyte. *Nature Communications*, 7: 1–8.
80. Faubert, P., Kondov, I., Qazzazie, D., Yurchenko, O. and Müller, C. (2018). A non-noble Cr-Ni-based catalyst for the oxygen reduction reaction in alkaline polymer electrolyte fuel cells. *MRS Communications*, *8*(1): 160-167.
81. Kabir, S., Lemire, K., Artyushkova, K., Roy, A., Odgaard, M., Schlueter, D. and Serov, A. (2017). Platinum group metal-free NiMo hydrogen oxidation catalysts: High performance and durability in alkaline exchange membrane fuel cells. *Journal of Materials Chemistry A*, 5(46): 24433-24443.
82. Xie, X., Liu, J., Li, T., Song, Y. and Wang, F. (2018). Post-formation copper-nitrogen species on carbon black: their chemical structures and active sites for oxygen reduction reaction. *Chemistry - A European Journal*, *24*(39): 9968-9975.
83. Hamedi, M., Wigenius, J., Tai, F. I., Björk, P. and Aili, D. (2010). Polypeptide-guided assembly of conducting polymer nanocomposites. *Nanoscale,* 2(10): 2058-2061.
84. Kang, Y. S., Heo, Y., Kim, P. and Yoo, S. J. (2017). Preparation and characterization of Cu–N–C electrocatalysts for oxygen reduction reaction in alkaline anion exchange membrane fuel cells. *Journal of Industrial and Engineering Chemistry*, 52(3): 35-41.

85. He, Q., Yang, X., Ren, X., Koel, B. E., Ramaswamy, N., Mukerjee, S. and Kostecki, R. (2011). A novel CuFe-based catalyst for the oxygen reduction reaction in alkaline media. *Journal of Power Sources*, 196(18): 7404-7410.
86. 86. Qiao, Y., Ni, Y., Kong, F., Li, R., Zhang, C., Kong, A. and Shan, Y. (2019). Pyrolytic carbon-coated Cu-Fe alloy nanoparticles with high catalytic performance for oxygen electroreduction. *Chemistry - An Asian Journal*, 14(15): 2676-2684.
87. Cui, L., Cui, L., Li, Z., Zhang, J., Wang, H., Lu, S. and Xiang, Y. (2019). A copper single-atom catalyst towards efficient and durable oxygen reduction for fuel cells. *Journal of Materials Chemistry A*, 7(28): 16690-16695.
88. Mosa, I. M., Biswas, S., El-Sawy, A. M., Botu, V., Guild, C., Song, W. and Suib, S. L. (2015). Tunable mesoporous manganese oxide for high performance oxygen reduction and evolution reactions. *Journal of Materials Chemistry A*, 4(2): 620-631.
89. Liu, J., Yu, M., Wang, X., Wu, J., Wang, C., Zheng, L. and Wang, W. (2017). Investigation of high oxygen reduction reaction catalytic performance on Mn-based mullite $SmMn_2O_5$. *Journal of Materials Chemistry A*, 5(39): 20922-20931.
90. Zhang, R., Zhang, J., Ma, F., Wang, W. Y. and Li, R. F. (2014). Preparation of Mn-N-C catalyst and its electrocatalytic activity for the oxygen reduction reaction in alkaline medium. *Ranliao Huaxue Xuebao/Journal of Fuel Chemistry and Technology*, 42(4): 467-475.
91. Stoerzinger, K. A., Risch, M., Han, B. and Shao-Horn, Y. (2015). Recent insights into manganese oxides in catalyzing oxygen reduction kinetics. *ACS Catalysis*, 5(10): 6021-6031.
92. Shao, Y., Liu, J., Wang, Y. and Lin, Y. (2009). Novel catalyst support materials for PEM fuel cells: Current status and future prospects. *Journal of Materials Chemistry*, 19(1): 46-59.
93. Qin, C., Wang, J., Yang, D., Li, B. and Zhang, C. (2016). Proton exchange membrane fuel cell reversal: A review. *Catalysts*, *6*(12), 197.
94. Chong, S. T., Lee, T. K., Samad, S., Loh, K. S., Wong, W. Y., Wan Daud, W. R. and Sunarso, J. (2018). Carbon and non-carbon support materials for platinum-based catalysts in fuel cells. *International Journal of Hydrogen Energy*, 43(16): 7823-7854.
95. Devrim, Y., Arıca, E. D. and Albostan, A. (2018). Graphene based catalyst supports for high temperature PEM fuel cell application. *International Journal of Hydrogen Energy*, 43(26): 11820-11829.
96. Khan, A. S. A., Ahmed, R. and Mirza, M. L. (2010). Performance evaluation of platinum-based catalysts for the development of proton exchange membrane fuel cells. *Turkish Journal of Chemistry*, 34(2): 193-206.
97. Choi, S. M., Seo, M. H., Kim, H. J. and Kim, W. B. (2011). Synthesis of surface-functionalized graphene nanosheets with high Pt-loadings and their applications to methanol electrooxidation. *Carbon*, 49(3): 904-909.
98. Suda, Y., Ozaki, M., Tanoue, H. and Takikawa, H. (2013). Supporting PtRu catalysts on various types of carbon nanomaterials for fuel cell applications. *Journal of Physics: Conference Series*, 433(1): 012008.
99. Molina-García, M. A. and Rees, N. V. (2016). Effect of catalyst carbon supports on the oxygen reduction reaction in alkaline media: A comparative study. *RSC Advances*, 6(97): 94669-94681.
100. Esfandiari, A. and Kazemeini, M. (2018). Investigating electrochemical behaviors of Ag@Pt core–shell nanoparticles supported upon different carbon materials acting as PEMFC’s cathodes. *Chemical Engineering Transactions*, 70: 2161-2166.
101. Minitha, C. R. and Rajendrakumar, R. T. (2013). Synthesis and characterization of reduced graphene oxide. *Advanced Materials Research*, 678: 56-60.
102. Kang, S. Y., Kim, H. J. and Chung, Y. H. (2018). Recent developments of nano-structured materials as the catalysts for oxygen reduction reaction. *Nano Convergence*, 5(1): 1-15.

103. Grigoriev, S. A., Fateev, V. N., Pushkarev, A. S., Pushkareva, I. V., Ivanova, N. A. and Kalinichenko, V. N., Wei, X. (2018). Reduced graphene oxide and its modifications as catalyst supports and catalyst layer modifiers for PEMFC. *Materials*, 11(8): 1405.
104. Alam, S. N., Sharma, N. and Kumar, L. (2017). Synthesis of graphene oxide (GO) by modified hummers method and its thermal reduction to obtain reduced graphene oxide (rGO). *Graphene*, 6(1): 118
105. Liu, J., Choi, H. J. and Meng, L. Y. (2018). A review of approaches for the design of high-performance metal/graphene electrocatalysts for fuel cell applications. *Journal of Industrial and Engineering Chemistry*, 64: 1-15.
106. Santoro, C., Serov, A., Stariha, L., Kodali, M., Gordon, J., Babanova, S. and Atanassov, P. (2016). Iron based catalysts from novel low-cost organic precursors for enhanced oxygen reduction reaction in neutral media microbial fuel cells. *Energy and Environmental Science*, 9(7): 2346-2353.
107. Soo, L. T., Loh, K. S., Mohamad, A. B., Daud, W. R. W. and Wong, W. Y. (2015). An overview of the electrochemical performance of modified graphene used as an electrocatalyst and as a catalyst support in fuel cells. *Applied Catalysis A: General*, 497: 198-210.
108. Xiao, M., Zhu, J., Feng, L., Liu, C. and Xing, W. (2015). Meso/macroporous nitrogen-doped carbon architectures with iron carbide encapsulated in graphitic layers as an efficient and robust catalyst for the oxygen reduction reaction in both acidic and alkaline solutions. *Advanced Materials*, 27(15): 2521-2527.
109. Liang, Y., Wang, H., Zhou, J., Li, Y., Wang, J., Regier, T. and Dai, H. (2012). Covalent hybrid of spinel manganese-cobalt oxide and graphene as advanced oxygen reduction electrocatalysts. *Journal of the American Chemical Society*, 134(7): 3517-3523.
110. Choi, H. J., Jung, S. M., Seo, J. M., Chang, D. W., Dai, L. and Baek, J. B. (2012). Graphene for energy conversion and storage in fuel cells and supercapacitors. *Nano Energy*, 1(4): 534-551.
111. Anastasopoulos, A., Blake, J. and Hayden, B. E. (2011). Non-noble intertransition binary metal alloy electrocatalyst for hydrogen oxidation and hydrogen evolution. *Journal of Physical Chemistry C*, 115(39): 19226-19230.
112. Osmieri, L. (2019). Transition metal–nitrogen–carbon (M–N–C) catalysts for oxygen reduction reaction. insights on synthesis and performance in polymer electrolyte fuel cells. *ChemEngineering*, 3(1): 16.
113. Li, L., Shen, S., Wei, G., Li, X., Yang, K., Feng, Q. and Zhang, J. (2019). A comprehensive investigation on pyrolyzed fe-n-c composites as highly efficient electrocatalyst toward the oxygen reduction reaction of PEMFCs. *ACS Applied Materials and Interfaces*, 11: 14126-14135.
114. Chen, Z., Higgins, D., Yu, A., Zhang, L. and Zhang, J. (2011). A review on non-precious metal electrocatalysts for PEM fuel cells. *Energy and Environmental Science*, 4(9): 3167-3192.
115. Ren, X., Lv, Q., Liu, L., Liu, B., Wang, Y., Liu, A. and Wu, G. (2019). Current progress of Pt and Pt-based electrocatalysts used for fuel cells. *Sustainable Energy and Fuels*, 4(1): 15-30.
116. Gautam, J., Huu Tuan, L., Kim, N. H., Van Hien, H., Thanh Tran, D., Lee, J. H. and Dinh Chuong, N. (2018). Emerging core-shell nanostructured catalysts of transition metal encapsulated by two-dimensional carbon materials for electrochemical applications. *Nano Today*, 22: 100-131.
117. Ansón-Casaos, A., Puértolas, J. A., Pascual, F. J., Hernández-Ferrer, J., Castell, P. and Benito, A. M., Martínez, M. T. (2014). The effect of gamma-irradiation on few-layered graphene materials. *Applied Surface Science*, 301: 264-272.
118. He, Y., Li, J., Li, L. and Li, J. (2016). Gamma-ray irradiation-induced reduction and self-assembly of graphene oxide into three-dimensional graphene aerogel. *Materials Letters*, 177(1): 76-79.
119. Abidin, Z., Muhamad, E., Ahmad Daud, N., Ibrahim, N., Chieng, B. and Talib, Z. (2017). Functionalizing graphene oxide with alkylamine by gamma-ray irradiation method. *Nanomaterials*, 7(6): 135.

120. Wang, W., Zhao, X., Shi, H., Liu, L., Deng, H., Xu, Z. and Miao, X. (2020). Shape inducer-free polygonal angle platinum nanoparticles in graphene oxide as oxygen reduction catalyst derived from gamma irradiation. *Journal of Colloid and Interface Science*, 575: 1-15.

121. Xu, Z., Chen, L., Zhou, B., Li, Y., Li, B., Niu, J. and Qian, X. (2013). Nano-structure and property transformations of carbon systems under γ-ray irradiation: A review. *RSC Advances*, 3(27): 10579-10597.

122. Park, H. Y., Yang, D. S., Bhattacharjya, D., Song, M. Y. and Yu, J. S. (2014). A highly efficient carbon-supported Pt electrocatalyst prepared by γ-irradiation for cathodic oxygen reduction. *International Journal of Hydrogen Energy*, 39(4): 1688-1697.

123. Meku, E., Du, C., Wang, Y. and Du, L. (2016). Impact of different synthesis methods on the electrocatalytic activity and stability of Pd-Fe/C nanoparticles for oxygen reduction reaction in fuel cells. *2016 International Conference on Engineering and Technology Innovations:* pp. 127-131.

124. Hung, T. F., Tu, M. H., Tsai, C. W., Chen, C. J., Liu, R. S., Liu, W. R. and Lo, M. Y. (2013). Influence of pyrolysis temperature on oxygen reduction reaction activity of carbon-incorporating iron nitride/nitrogen-doped graphene nanosheets catalyst. *International Journal of Hydrogen Energy*, 38(10): 3956-3962.

125. Jeon, M. K. and McGinn, P. J. (2012). Co-alloying effect of Co and Cr with Pt for oxygen electro-reduction reaction. *Electrochimica Acta*, *64*(3): 147-153.

126. Sharin, S., Rahman, I. A., Ahmad, A. F., Mohd, H. M. K., Mohamed, F., Radiman, S., … and Bastamam, I. S. A. (2015). Penurunan grafin oksida kepada grafin menggunakan sinar gama. *Malaysian Journal of Analytical Sciences*, 19(6): 1223-1228.

127. Li, Z., Yang, Y., Relefors, A., Kong, X., Siso, G. M., Wickman, B. and Soroka, I. L. (2021). Tuning morphology, composition and oxygen reduction reaction (ORR) catalytic performance of manganese oxide particles fabricated by γ-radiation induced synthesis. *Journal of Colloid and Interface Science*, 583: 71-79.

128. Mashentseva, A. A., Shlimas, D. I., Kozlovskiy, A. L., Zdorovets, M. V., Russakova, A. V., Kassymzhanov, M. and Borisenko, A. N. (2019). Electron beam induced enhancement of the catalytic properties of ion-track membranes supported copper nanotubes in the reaction of the P-nitrophenol reduction. *Catalysts*, 9(9): 737.

129. Kakitani, K., Kimata, T., Yamaki, T., Yamamoto, S., Shimoyama, I., Matsumura, D. and Terai, T. (2017). Activity enhancement of platinum nanoparticle catalysts on ion-beam-irradiated carbon support. *National Institutes for Quantum and Radiological Science and Technology*, 34: 2016-2018.

130. Nakagawa, N., Ishitobi, H., Abe, S., Kakinuma, M., Koshikawa, H., Yamamoto, S. and Yamaki, T. (2019). A novel method to enhance the catalytic activity of PtRu on the support using CeO_2 by high-energy ion-beam irradiation. *Catalysis Today*, 364: 118-124.

131. Choi, Y., Lim, D., Oh, E., Lim, C. and Baeck, S. H. (2019). Effect of proton irradiation on electrocatalytic properties of MnO_2 for oxygen reduction reaction. *Journal of Materials Chemistry A*, 7(19): 11659-11664.

132. Ohkubo, Y., Hamaguchi, Y., Seino, S., Nakagawa, T., Kageyama, S., Kugai, J. and Yamamoto, T. A. (2013). Preparation of carbon-supported PtCo nanoparticle catalysts for the oxygen reduction reaction in polymer electrolyte fuel cells by an electron-beam irradiation reduction method. *Journal of Materials Science*, 48(14): 5047-5054.